ACS APPLIED MATERIALS & INTERFACES

Research Article

www.acsami.org

# Ecological Approach to Graphene Oxide Reinforced Poly (methyl methacrylate) Nanocomposites

Seira Morimune,[†] Takashi Nishino,*[,†] and Takuya Goto[‡]

[†]Department of Chemical Science and Engineering, Graduate School of Engineering, Kobe University, Rokko, Nada, Kobe, 657-8501 Japan

[‡]Mitsubishi Gas Chem. Inc., Niijuku, Katsushika, Tokyo, 125-8601 Japan

Supporting Information

**ABSTRACT:** Graphene oxide (GO) possesses the desirable characteristic of aqueous solution processability attributed to the oxygen-containing functional groups on the basal planes and edges of graphene. To provide an alternative to conventional procedures for fabricating poly (methyl methacrylate) (PMMA)/GO nanocomposites, which use organic solutions and/or surfactants, we have developed an environmentally friendly technique in which PMMA is polymerized by soap-free emulsion polymerization and incorporated with GO using water as a processing medium. Experimental results showed that the fabricated PMMA/GO nanocomposites had excellent mechanical, thermal, and $O_2$ barrier properties with the nanodispersion of GO.

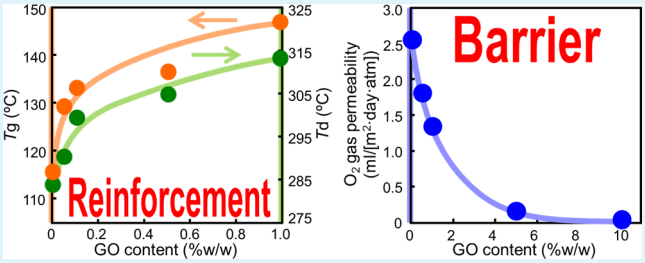


**KEYWORDS:** *nanocomposites, graphene oxide, poly (methyl methacrylate), soap-free emulsion polymerization, environmentally-friendly, mechanical properties*

## 1. INTRODUCTION

Graphene, which consists of a single layer of $sp^2$-bonded carbon atoms, has been one of the most in-demand materials of the past decade. In the past, several approaches to synthesize the monolayer of graphene have been reported, including epitaxial growth on single-crystal SiC,[1] direct growth on single-crystal metal film[2−4] or polycrystalline film[5−7] through chemical vapor deposition, and chemical reduction of exfoliated graphene oxide layers.[8−10] In 2004, Geim et al. proposed mechanical exfoliation from graphite using Scotch tape.[11] They later were awarded the Nobel prize in physics in 2010, and both academic and industrial interest in graphene exploded. An enormous amount of research on graphene has been conducted, and its excellent mechanical, thermal, and electrical properties have been revealed. With its Young's modulus of 1 TPa, ultimate strength of 130 GPa, and the thermal conductivity of 5000 W/mK, graphene is clearly one of the most promising materials for developments in nanotechnology across many fields.[12,13] Graphene oxide (GO), a functionalized graphene material, bears oxygen-containing functional groups on the basal planes and edges of graphene. These groups attach the characteristics of aqueous solution processability (such as water dispersibility) to the pristine graphene.[14] GO can be prepared by a simple and cheap process in any laboratory; in addition, GO shows high performances similar to those of graphene.[15]

In the past, polymer nanocomposites reinforced by carbon-based nanomaterials such as carbon nanotubes (CNTs) have often been reported.[16−18] CNTs have been considered potential candidates for many applications in nanotechnology due to their very high aspect ratio and unique electrical, thermal, and mechanical properties. However, CNTs tend to bundle together and form macro/microaggregates in polymer matrixes, which can cause defects in the material. Many efforts have been made to improve the dispersibility of CNTs in polymer matrixes: for example, by the surface modification of CNTs.[19−23] In this respect, GO is an effective nanofiller of polymer nanocomposites due to its aqueous solution processability (which enables GO to be nanodispersed in the polymer matrixes by simple processes) combined with the excellent properties that are characteristic of all carbon-based nanomaterials. Moreover, the nanodispersion of the anisotropic structure of GO, as well as clay, is expected to significantly improve the properties because of its high aspect ratio and the surface area. Therefore, the development of GO/polymer nanocomposites has attracted a great deal of attention among researchers all over the world.

So far, many groups have reported on GO reinforced polymer nanocomposites using hydrophilic polymer, such as poly (ethylene oxide) or poly (vinyl alcohol) (PVA).[24,25] We ourselves have revealed the excellent reinforcement effect of GO in PVA/GO nanocomposites.[25] Nanocomposites with GO have also been produced using hydrophobic polymer, including polystyrene (PS), polyurethane (PU), and poly (methyl methacrylate) (PMMA).[26]

Received: April 16, 2012
Accepted: June 13, 2012
Published: June 13, 2012

  

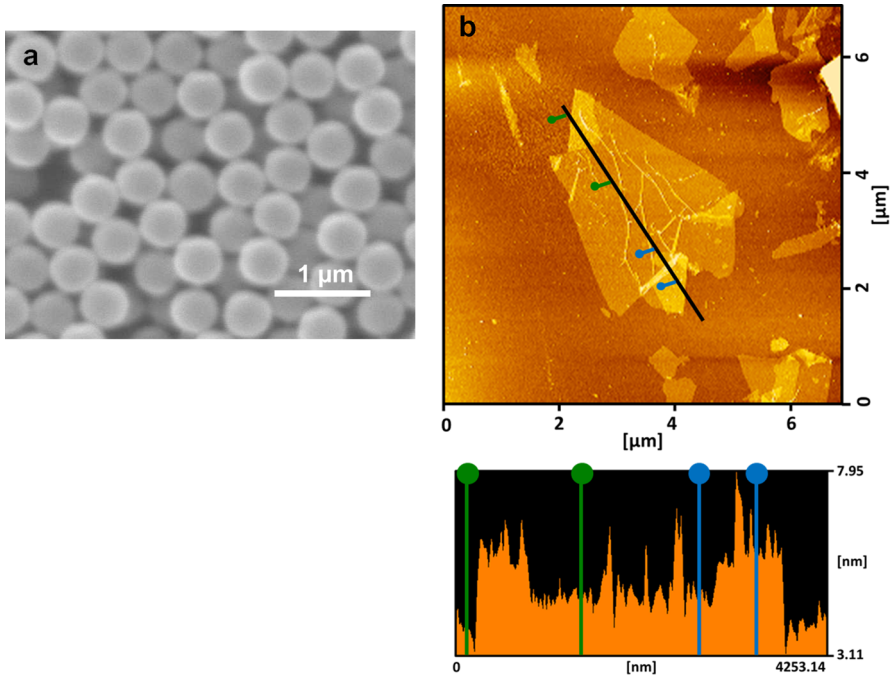


**Figure 1.** (a) SEM photograph of PMMA particles. (b) AFM image and height profile of GO.

There are several procedures for preparing PMMA/GO nanocomposites. For example, they have been prepared by dissolving PMMA using an organic solvent such as dimethylformamide mixed with GO powder under vigorous stirring. PMMA/GO suspension has been fabricated into films by the casting method, vacuum-assisted self-assembly, and the layer-by-layer method.[27−30] PMMA/GO nanocomposites have also been prepared by in situ polymerization.[31,32] However, the organic solvents and surfactants used in these processes are harmful to the environment.

Here, we propose a new, environmentally friendly process for the preparation of PMMA/GO nanocomposites. Instead of the use of the organic solvent/surfactant combination, we mix PMMA from soap-free emulsion polymerization with GO aqueous suspension. This simple and environmentally friendly process enables the GO to be dispersed in the PMMA homogeneously. Furthermore, it is easy to control a wide range of GO content. We also found that the resultant PMMA/GO nanocomposites had excellent enhancements of their mechanical, thermal, and $O_2$ barrier properties.

## 2. EXPERIMENTAL SECTION

**2.1. Materials.** GO aqueous suspension with a content of 1% w/w was supplied by Mitsubishi Gas Chemical Inc. GO was synthesized from graphite using the Huhmmers' method.[8] Methyl methacrylate monomer (MMA, Sigma Aldrich) was distilled under nitrogen at reduced pressure. Potassium peroxydisulfate (KPS, Sigma Aldrich), the initiator, was recrystallized and dried in vacuum. Hydrochloric acid (HCl, Sigma Aldrich) was used as supplied.

**2.2. Sample Preparation.** *PMMA.* First, we performed soap-free emulsion polymerization. Distilled water (300 g), MMA monomer (50 g), and KPS (0.5% w/w vs MMA) was sequentially added to the flask. The mixture was then stirred at 330 rpm at 70 °C for 12 h. The emulsion was stabilized by the electric hindrance through the sulfate groups on the particle surface against coagulation.[33] The diameter of the PMMA particles was 450 ± 20 nm (Figure 1a), and the particles were observed with a scanning electron microscope (SEM) (TSM-5610LVS, JEOL) at an accelerating voltage of 10 kV. Pt/Pd was deposited on the sample surface prior to observation. The average molecular weight of the PMMA was 440 000 (the degree of polymerization = 4400), which was analyzed as solutions in chloroform of 0.5% w/w by gel permeation chromatography (HITACHI L-7000 Series, Hitachi Ltd.) and detected with a refractive index spectrometer (HITACHI L-7490, Hitachi Ltd.). The TSKgel GMHHR-M column (Tosoh Corp.) was used with the flow rate of 1 mL/min at 30 °C. The molecular weight was calibrated with monodisperse polystyrene standards.

*PMMA/GO Nanocomposites.* GO aqueous suspension (1% w/w) was added to the PMMA emulsion and stirred for 1 day. Subsequently, 1% w/w HCl aqueous solution was added dropwise to the mixture while stirring. The coaggregated precipitant of PMMA/GO was rinsed with distilled water and dried in the oven at 50 °C and then in vacuum at 40 °C. PMMA/GO powder was melt-pressed at 180 °C for 15 min under 6 MPa. The amount (0−10% w/w vs PMMA) of the GO content in the nanocomposite was adjusted by changing the amount of GO aqueous suspension added.

**2.3. Characterization.** Atomic force microscopic (AFM) analysis was performed on the GO with a NanoNavi Station/E-sweep (Seiko Instruments). A silicon cantilever probe was used in the tapping mode in air. The GO aqueous suspension was diluted with distilled water and spin-coated on a silicon wafer. X-ray diffraction of GO, PMMA, and the nanocomposites was performed with an X-ray diffractometer (RINT2100, Rigaku) using Ni-filtered Cu K$\alpha$ radiation and operated at 40 kV and 20 mA. The $2\theta/\theta$ scan data were collected at 0.02 degree intervals with a scanning speed of 1.0 degree/min.

The tensile test was conducted using an Autograph AGS-1kND (Shimadzu) with a cross head speed of 2 mm/min. More than ten specimens were tested with the initial length of 20 mm. The toughness ($K$), equal to the area surrounded by the stress ($\sigma$)−strain ($\varepsilon$) curve, was calculated as

$$K = \int_{\varepsilon=0}^{\varepsilon=\varepsilon_{max}} \sigma \cdot d\varepsilon / d \quad (\mathrm{J/g}) \tag{1}$$

where $\sigma$ is the stress (Pa), $\varepsilon$ is the strain, and $d$ is the density (g/m$^3$). For statistics, these experiments were performed for at least 10 different specimens in different days; then, averaged values and their standard deviations of Young's modulus, tensile strength, elongation at break, and toughness were calculated. Dynamic mechanical analyses (DMAs) were carried out using a dynamic mechanical analyzer (DVA-220S, ITK). The rectangular shaped specimen was heated at a heating


dx.doi.org/10.1021/am3006687 | ACS Appl. Mater. Interfaces 2012, 4, 3596−3601

rate of 6 °C/min, and a frequency of 10 Hz was set under nitrogen flow. The measurement was conducted during the first heating process, and at least five specimens were tested for each specimen.

The thermal decomposition temperature ($T_d$) was measured by a thermogravimeter (TG) (TG/DTA-220CU, Seiko Instruments) at a heating rate of 10 °C/min under nitrogen flow. $T_d$ was defined as a temperature of 5% thermal weight loss. $O_2$ gas permeability was measured at 25 °C and relative humidity of 50% on an OX-TRAN 2/21 (MOCON). The thickness of the specimens was 1 mm.

## 3. RESULTS AND DISCUSSION

**3.1. Characterization.** Figure 1b shows the AFM image and the height profile of the GO along the line. The GO sheet had an irregular form, with some wrinkles and folding on the surface and edge. Judging from the height profile, the GO thickness was 0.8−1.0 nm with an average aspect ratio of 3000. It is apparent that the GO sheets are fully exfoliated and dispersed as monolayers in the aqueous suspension. The Fourier transform infrared spectrum and X-ray photoelectron spectrum show that the GO surface is adequately oxidized with the presence of hydroxyl, carbonyl, carboxyl, and epoxy groups. The details are shown in the Supporting Information (Supporting Figure 1a−c, Supporting Table 1).

Figure 2 shows X-ray diffraction profiles of the PMMA, PMMA/GO nanocomposites, and GO. The GO was dried

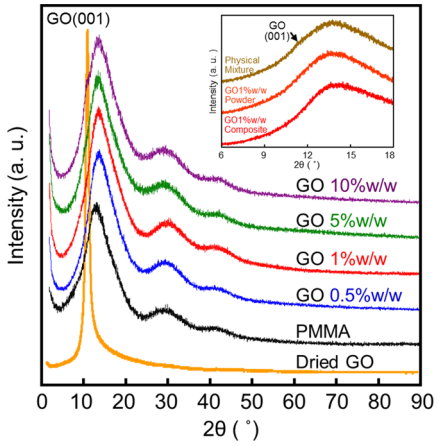


**Figure 2.** X-ray diffraction profiles of PMMA film, PMMA/GO nanocomposites, and GO.

from the aqueous suspension. On the GO profile, the characteristic peak of 001 reflection corresponding to the GO interlayer appeared clearly at $2\theta = 10.1°$. The presence of this reflection indicates that the GO sheets stacked themselves on top of each other and became graphite-like during the simple drying procedure. PMMA showed the diffuse scattering typical of amorphous polymer. On the profiles of the nanocomposites with 5 and 10% w/w GO loadings, the 001 reflection appeared to overlap with the scattering of PMMA. We conclude that the excess amount of GO caused the strong interaction between the GO sheets themselves and the formation of agglomerates in the polymer matrix. In contrast, for the nanocomposites with a low content of GO (up to 1% w/w), the 001 reflection disappeared, which reveals the exfoliation and nanodispersion of GO into the PMMA matrix.[34] Similar to the low content nanocomposites, as shown in the corner of the profiles, the 001 reflection of the GO interlayer was not observed for the dried coaggregated precipitant of PMMA/GO with 1% w/w GO loading, though it was detected for the physical mixture of the PMMA powder and 1% w/w of GO powder. This suggests that the mixing of PMMA and GO in the presence of water is necessary for the nanodispersion of GO.

**3.2. Mechanical Properties.** Figure 3a shows the typical stress ($\sigma$)−strain ($\varepsilon$) curves of the PMMA film and the PMMA/GO nanocomposites. The Young's modulus ($E$) of the nanocomposites dramatically increased when GO was incorporated. As for 1%w/w GO loading, the $E$ value (4.1 GPa) was double that of PMMA (2.2 GPa). We attribute this result to the expected exfoliated structure of the GO in the nanocomposites. The high aspect ratio of the GO was effectively imparted to the nanocomposites with their rigid structure. Figure 3b shows the effect of GO loading on the $E$, tensile strength ($\sigma_{max}$), elongation at break ($\varepsilon_{max}$), and the toughness ($K$) of the PMMA film and the PMMA/GO nanocomposites with standard deviations (see also Supporting Table 2, Supporting Information). Typically, there are a few problems with the mechanical properties of polymer nanocomposites reinforced using rigid fillers. When stress is applied to the nanocomposite, the stress concentrates at the interface of the matrix/filler and the craze occurs and the crack propagates, which results in the destruction of the entire composite. Therefore, although an increase in the $E$ and $\sigma$ values has often been reported, there were few reports for the increase in the $\varepsilon$ value or the $K$ value in previous studies.[35] The improvement of this issue has been requisite. In contrast, the $\varepsilon$ value of the PMMA/GO nanocomposites remained almost the same as that of the PMMA film. As a result, the $K$ value increased up to 35% compared with that of the PMMA film. We can thus conclude that GO plays a role in the crack pinning of nanocomposites. Figure 3c,d shows the SEM photographs of the cross section of the PMMA and the PMMA/GO nanocomposites, respectively, after fracture. The PMMA had a conchoidal fracture, which is typical for amorphous glassy polymer, while the nanocomposite had a scaly pattern, which is completely different from the PMMA. This indicates that, in the nanocomposite, the GO was what prevented the crack propagation. These results show that our proposed fabrication process could successfully achieve the nanodispersion of GO with a low content. The $\varepsilon$ value decreased drastically when more GO was added to the polymer matrix, a result that we attribute to the brittleness of the GO agglomerates. The interactions between the GO sheets, mainly by van der Waals force, stacked the sheets together and formed GO agglomerates. These agglomerates reduced the aspect ratio of the filler and easily caused the fracture at the interface between the polymer matrix and the agglomerates. Therefore, the $\varepsilon$ and $\sigma$ values of the nanocomposites with GO loading of 5 and 10% w/w decreased.

Figure 4a,b shows the temperature dependence of the storage modulus ($E'$) and the mechanical tan $\delta$ of the PMMA film and the PMMA/GO nanocomposites, respectively. The main dispersion in tan $\delta$, so-called $\alpha_a$, in the region from 100 to 150 °C is assigned as the glass transition temperature ($T_g$). It is apparent that the peak of the $\alpha_a$ dispersion largely shifted to the higher temperature and the intensity decreased by the incorporation of GO. With only 1% w/w GO loading, an increase of 30 °C was observed for the nanocomposite (Figure 4d, Supporting Table 3, Supporting Information). The increase in $T_g$ is attributed to the restriction of the mobility of the PMMA chains' interaction with the nanodispersed GO sheets. This also appeared as the decrease in the $E'$ value over the $T_g$ was suppressed. Within the entire temperature range (−150 to 200 °C), the high $E'$ value was maintained for the PMMA/GO

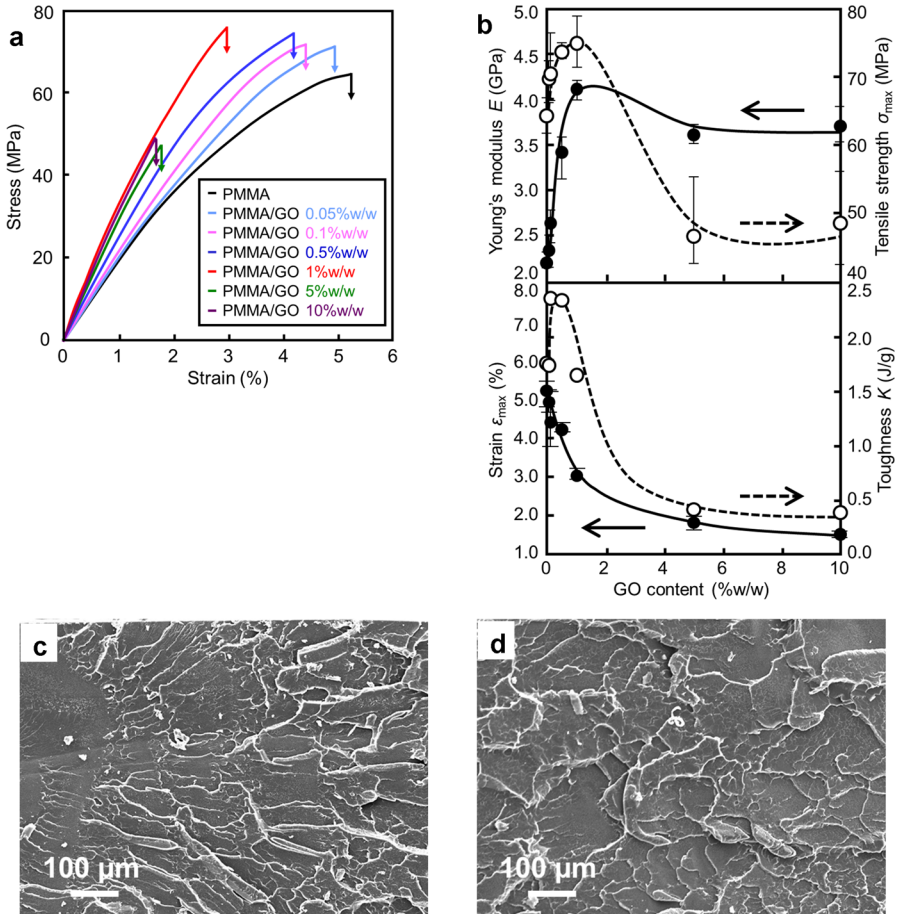


**Figure 3.** (a) Stress–strain curves of PMMA film and PMMA/GO nanocomposites. (b) Experimental Young's modulus ($E$), tensile strength ($\sigma_{max}$), strain ($\varepsilon_{max}$), and toughness ($K$) of the PVA/GO nanocomposites. SEM photographs of the cross section of (c) PMMA and (d) PMMA/GO nanocomposite (1%w/w) after fracture.

nanocomposites. This indicates that GO functions as an excellent reinforcing filler.

**3.3. Thermal Properties.** Figure 4c shows the TG traces of PMMA film and PMMA/GO nanocomposites. There was a definite enhancement in the thermal degradation temperature ($T_d$) by the incorporation of GO. Figure 4d shows the relationship between $T_d$ and the GO content. The $T_d$ of the nanocomposites increased linearly with the addition of GO up to 1% w/w loading. A 28 °C increase in $T_d$ can be observed with only 1% w/w of GO content (Supporting Table 3, Supporting Information). This suggests that GO acts as a barrier to hinder the volatile decomposition products throughout the composites.

**3.4. Barrier Properties.** Improvement in the barrier properties has often been reported for many kinds of polymer/clay nanocomposites.[36−38] Exfoliated clay with a high aspect ratio and effective surface area in the matrix widens the pathway for the permeating gas molecules. The strategy for improving the barrier properties can also be expected to work for the PMMA/GO nanocomposites because of the exfoliated morphology of the GO.

Figure 5 shows the $O_2$ gas permeability of the PMMA film and the PMMA/GO nanocomposites. Tsai et al.[39] reported a 50% reduction of the gas permeability by the 5% w/w incorporation of clay into PMMA. However, in this study, it was obvious that the $O_2$ gas permeability was significantly suppressed with the addition of GO: the addition of only 1% w/w of GO to the PMMA matrix decreased the permeability by 50%. Furthermore, the nanocomposite with 10% w/w of GO was found to be almost completely impermeable. In the PMMA/GO nanocomposites, the nanodispersion of GO with its high aspect ratio achieved the high performance in the barrier properties.

## 4. CONCLUSIONS

We proposed a new method of preparing PMMA/GO nanocomposites using an aqueous medium. The proposed method can be used to prepare nanocomposites with a wide range of GO content, rather than the two extremes, low or high, it had been limited to before. This technique is practical for use in a wide variety of industries.

In the nanocomposites, GO was highly exfoliated and nanodispersed. Results of tensile testing showed that the nanocomposites maintained the elongation of the matrix in spite of the incorporation of a rigid filler. Therefore, not only the $E$ and $\sigma$ values but also the $K$ value increased. The nanocomposites demonstrated high barrier properties, which we attribute to the high aspect ratio of GO. The nanocomposites with 10% w/w GO loading were almost completely impermeable. Furthermore, a remarkable enhancement in the $T_g$ and $T_d$ was observed by the incorporation of GO. Overall, not only excellent properties but also the unique morphology of GO was successfully imparted to the PMMA/GO nanocomposites.


dx.doi.org/10.1021/am3006687 | ACS Appl. Mater. Interfaces 2012, 4, 3596−3601

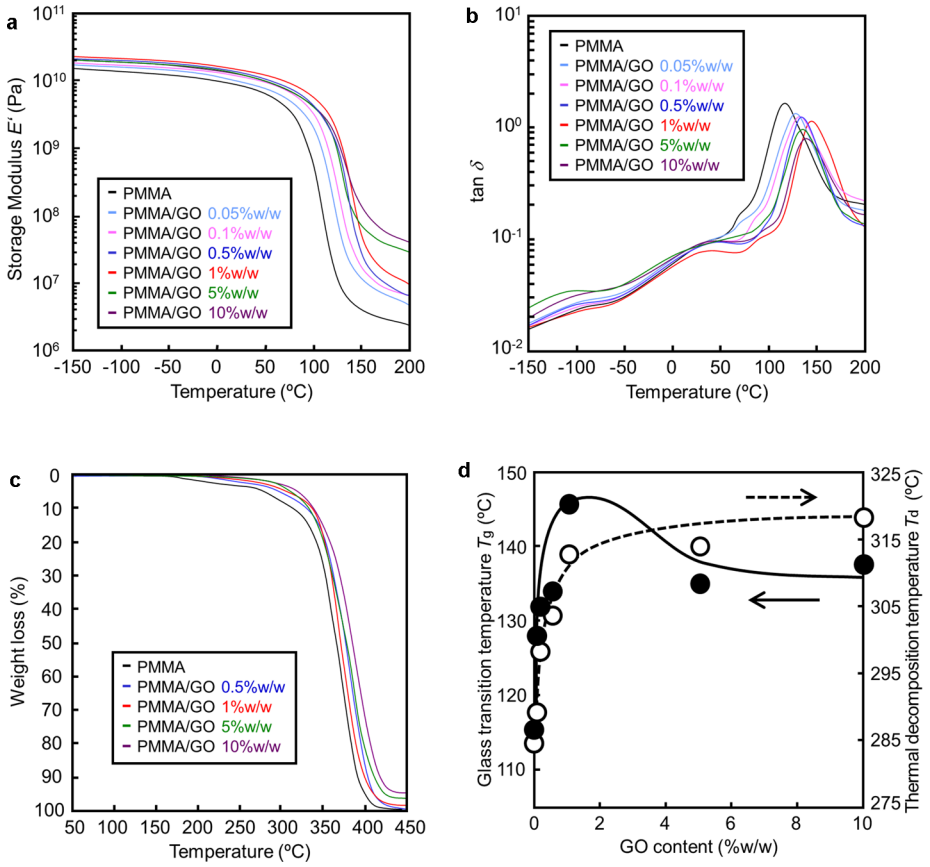


**Figure 4.** Temperature dependence of (a) storage modulus ($E'$) and (b) tan $\delta$ of PMMA film and PMMA/GO nanocomposites. (c) Thermogravimetric traces of PMMA film and PMMA/GO nanocomposites. (d) Relationships between glass transition temperature ($T_g$), thermal degradation temperature ($T_d$), and GO content.

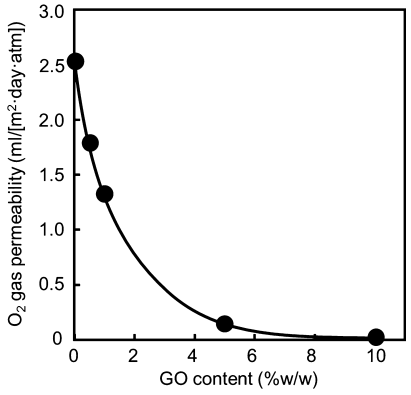


**Figure 5.** $O_2$ gas permeability of PMMA film and PMMA/GO nanocomposites.

## ■ ASSOCIATED CONTENT

### Supporting Information

FT-IR spectrum and XPS analyses of GO, tables summarizing mechanical and thermal properties of PMMA/GO nanocomposites. This material is available free of charge via the Internet at http://pubs.acs.org

## ■ AUTHOR INFORMATION

### Corresponding Author

*Tel: 81-78-803-6164. Fax: 81-78-803-6198. E-mail: tnishino@kobe-u.ac.jp.

### Notes

The authors declare no competing financial interest.

## ■ REFERENCES

(1) Berger, C.; Song, Z.; Li, X.; Wu, X.; Brown, N.; Naud, C.; Mayou, D.; Li, T. B.; Hass, J.; Marchenkov, A. N.; Conrad, E. H.; First, P. N.; Heer, W. A. *Science* **2006**, *312*, 1191.
(2) Sutter, P. W.; Flege, J. I.; Sutter, E. A. *Nat. Mater.* **2008**, *7*, 406.
(3) Coraux, J.; N'Diaye, A. T.; Busse, C.; Michely, T. *Nano Lett.* **2008**, *8*, 565.
(4) Parga, A. L. V.; Calleja, F.; Borca, B.; Passeggi, M. C. G.; Hinarejos, J. J.; Guinea, F.; Miranda., R. *Phys. Rev. Lett.* **2008**, *100*, 056807.
(5) Yu, Q.; Lian, J.; Siriponglert, S.; Li, H.; Chen, Y. P.; Pei, S. S. *Appl. Phys. Lett.* **2008**, *93*, 113103.
(6) Kim, K. S.; Zhao, Y.; Jang, H.; Lee, S. Y.; Kim, J. M.; Kim, K. S.; Ahn, J. H.; Kim, P.; Choi, J. Y.; Hong, B. H. *Nature* **2009**, *457*, 706.
(7) Reina, A.; Jia, X; Ho, J.; Nezich, D.; Son, H.; Bulovic, V.; Dresselhaus, M. S.; Kong., J. *Nano Lett.* **2009**, *9*, 30.
(8) Hummers, W. S.; Offeman, R. E. *J. Am. Chem. Soc.* **1958**, *80*, 1339.
(9) Becerril, H. A.; Mao, J.; Liu, Z.; Stoltenberg, R. M.; Bao, Z.; Chen, Y. *ACS Nano* **2008**, *2*, 463.
(10) Yang, D.; Velamakanni, A.; Bozoklu, G.; Park, S.; Stoller, M.; Piner, D.; Stankovich, S.; Jung, I.; Field, D. A.; Ventrice, C. A.; Ruoff, R. S. *Carbon* **2009**, *47*, 145.
(11) Novoselov, K. S.; Geim, A. K.; Morozov, S. V.; Jiang, D.; Zhang, Y.; Dubonos, S. V.; Grigorieva, I. V.; Firsov, A. A. *Science* **2004**, *306*, 666.
(12) Lee, C.; Wei, X.; Kysar, J. W.; Hone, J. *Science* **2008**, *321*, 385.

(13) Balandin, A. A.; Ghosh, S.; Bao, W.; Calizo, I.; Teweldebrhan, D.; Miao, F.; Lau, C. N. *Nano Lett.* **2008**, *8*, 902.
(14) Rourke, J. P.; Pandey, P. A.; Moore, J. J.; Bates, M.; Kinloch, I. A.; Young, R. J.; Wilson, N. R. *Angew. Chem., Int. Ed.* **2011**, *50*, 3173.
(15) Wilson, N. R.; Pandey, P. A.; Beanland, R.; Young, R. J.; Kinloch, I. A.; Gong, L.; Liu, Z.; Suenaga, K.; Rourke, J. P.; York, S. J.; Sloan, J. *ACS Nano* **2009**, *3*, 2547.
(16) Iijima, S. *Nature* **1991**, *354*, 56.
(17) Baughman, R. H.; Zakhidov, A. A.; Heer, W. A. *Science* **2002**, *279*, 787.
(18) Morimune, S.; Kotera, M.; Nishino, T.; Goto, K.; Hata, K. *Macromolecules* **2011**, *44*, 4415.
(19) Gong, X.; Liu, J.; Baskaran, S.; Voise, R.; Young, J.; James, S. *Chem. Mater.* **2000**, *12*, 1049.
(20) Velasco, C.; Martinez, A. L.; Lozada, M.; Alvarez, M.; Castaño, V. M. *Nanotechnology* **2002**, *13*, 495.
(21) Gojny, H.; Nastalczyk, J.; Roslaniec, Z.; Schulte, K. *Chem. Phys. Lett.* **2003**, *370*, 820.
(22) Moniruzzaman, M.; Winey, K. I. *Macromolecules* **2006**, *39*, 5194.
(23) Trujillo, M.; Arnal, M. L.; Müller, A. J. *Macromolecules* **2007**, *40*, 6268.
(24) Hirata, M.; Gotou, T.; Horiuchi, S.; Fujiwara, M.; Ohba, M. *Carbon* **2004**, *42*, 2929.
(25) Morimune, M.; Nishino, T.; Goto, T. *Polym. J.*, DOI:10.1038/pj.2012.58.
(26) Kim, H.; Abdala, A. A.; Macosko, W. *Macromolecules* **2010**, *43*, 6515.
(27) Bao, Q.; Zhang, H.; Yang, J.; Wang, S.; Tang, D. Y.; Jose, R.; Ramakrishna, S. C.; Lim, T.; Loh, K. P. *Adv. Funct. Mater.* **2010**, *20*, 782.
(28) Wang, W. P.; Pan, C. Y. *Polym. Eng. Sci.* **2004**, *44*, 2335.
(29) Zhang, H. B.; Yan, Q.; Zheng, W. G.; He, Z.; Yu, Z. Z. *ACS Appl. Mater. Interfaces* **2011**, *3*, 918.
(30) Putz, K. W.; Compton, O. C.; Palmeri, M. J.; Nguyen, S. T.; Brinson, L. C. *Adv. Funct. Mater.* **2010**, *20*, 3322.
(31) Jang, J. Y.; Kim, M. S.; Jeong, H. M.; Shin, C. M. *Compos. Sci. Technol.* **2009**, *69*, 186.
(32) Xu, Y.; Hong, W.; Bai, H.; Li, C.; Shi, G. *Carbon* **2009**, *47*, 3538.
(33) Okubo, M.; Yamada, A.; Shibao, S.; Nakamae, K.; Matsumoto, T. *J. Appl. Polym. Sci.* **1981**, *26*, 1675.
(34) Liang, J.; Houng, Y.; Zhang, L.; Wang, Y.; Ma, Y.; Guo, T.; Chen, Y. *Adv. Funct. Mater.* **2009**, *19*, 2297.
(35) Usuki, A.; Hasegawa, N.; Kadoura, H.; Okamoto, T. *Nano Lett.* **2001**, *1*, 271.
(36) Morimune, S.; Kotera, M.; Nishino, T. *J. Adhes. Soc. Jpn.* **2010**, *46*, 320.
(37) Russo, G. M.; Simon, G. P.; Incarnato, L. *Nano Lett.* **2010**, *10*, 4970.
(38) Morgan, A. P.; Gamboa, D.; Holder, K. M.; Grunlan, J. C. *Langmuir* **2011**, *27*, 12106.
(39) Tsai, T. Y.; Lin, M. J.; Chang, C. W.; Li, C. C. *J. Phys. Chem. Solids* **2010**, *71*, 590.